Journal of Plant Growth Regulation
https://doi.org/10.1007/s00344-026-12331-8

AMF and *Trichoderma* Confer Cereal Cyst Nematode '*Heterodera filipjevi*' Resistance in Wheat by Fine-tuning Ionomics, Metabolomics, and Transcriptomics

Özgenur Arslanoğlu[1] · Muhammad Sameeullah[2] · Ayşegül Yaman[1] · Nagihan Duman[1] · Furkan Ulaş[3] · Ebubekir Yüksel[4] · Mustafa İmren[1] · Abdelfattah A. Dababat[5]

Received: 4 December 2025 / Accepted: 26 June 2026
© The Author(s), under exclusive licence to Springer Science+Business Media, LLC, part of Springer Nature 2026

Abstract

Cereal cyst nematodes (CCNs, *Heterodera filipjevi*) are major constraints to global wheat productivity. Beneficial microbes such as arbuscular mycorrhizal fungi (AMF) and *Trichoderma* are known to enhance plant stress tolerance, yet their combined effects on CCN resistance in wheat remain largely unexplored. This study investigated the individual and synergistic roles of AMF and *Trichoderma* in conferring resistance to *H. filipjevi* in the susceptible wheat cultivar Bezostaya using integrated ionomics, metabolomics, and transcriptomics approaches. The combined AMF + *Trichoderma* treatment most effectively suppressed CCN populations (reproduction factor: 1.17) compared with the untreated control (4.50) and single-agent treatments. Successful root colonization by both symbionts was confirmed. Ionomic profiling revealed synergistic enhancement of nitrate, potassium, iron, manganese, and zinc uptake, suggesting improved nutritional status and stress resilience. Metabolomic analysis identified significant elevation of 2-descarboxy-betanidin and reduction of N-(3-acetamidopropyl)-4-aminobutanal in combined-treatment plants, with additional shifts in defense-related amino acids and secondary metabolites supporting antimicrobial biosynthesis. Transcriptomic profiling revealed 1,110 upregulated and 1,718 downregulated genes. Key upregulated defense genes included *PRB1-2*, *PRB1-3*, *RPM1*, *BTB* domain-containing protein, *MAPK kinase substrate protein*, and *cinnamoyl-CoA reductase 1-like*, reflecting activation of salicylic acid-mediated immunity, MAPK cascades, and hormone signaling. Downregulated pathways included phenylpropanoid biosynthesis and starch/sucrose metabolism. Promoter analysis of *PRB1-2* confirmed cis-elements responsive to symbiosis and pathogen elicitors, and subcellular localization confirmed its apoplastic defense role. The synergistic AMF–*Trichoderma* consortium orchestrates a robust, multi-layered defense response, offering significant potential for sustainable nematode management and improved wheat productivity.

Keywords Wheat · *H. filipjevi* · AMF · *Trichoderma* · Pathogenesis-related genes · Transcriptomics

Communicated by Barry Flinn

✉ Muhammad Sameeullah
sameepbg@gmail.com

✉ Mustafa İmren
m.imren37@gmail.com

✉ Abdelfattah A. Dababat
A.Dababat@cgiar.org

[1] Faculty of Agriculture, Department of Plant Protection, Bolu Abant Izzet Baysal University, Bolu, Turkey

[2] Faculty of Agriculture, Department of Field Crops, Bolu Abant Izzet Baysal University, Bolu, Turkey

[3] Department of Plant Protection, Faculty of Agricultural Sciences and Technology, Sivas University of Science and Technology, Sivas, Turkey

[4] Department of Plant Protection, Faculty of Agriculture, Erciyes University, Kayseri, Turkey

[5] International Maize and Wheat Improvement Centre (CIMMYT), P.K. 39, Emek, Ankara 06511, Turkey

Published online: 11 July 2026

Introduction

Small-grain cereals have served as the basis for staple foods, beverages, and animal feed for thousands of years (Breiman and Graur 1995; Gustafson et al. 2009). Wheat (*Triticum aestivum*) is the second most produced cereal crop after maize and is rich in calories, proteins, carbohydrates, vitamins, and minerals. However, wheat productivity is strongly influenced by both biotic and abiotic factors. Diseases and pests, together with drought, heat, and soil salinity, can substantially reduce wheat yield and quality. Among biotic constraints, plant-parasitic nematodes (PPNs) are among the most destructive pests affecting global crop production and cause significant economic losses annually. Cereal cyst nematodes (CCNs, *Heterodera* spp.) are among the most important PPNs limiting the production of small-grain cereals. Heavily invaded young plants are stunted, and their lower leaves are often chlorotic, forming pale green patches in the field. Mature plants also show reduced tillering, stunting, and shallow roots with a "bushy-knotted" appearance (Smiley et al. 2017).

In recent years, increasing attention has been given to biological control agents, particularly beneficial microorganisms such as arbuscular mycorrhizal fungi (AMF) and *Trichoderma* spp., as eco-friendly approaches to mitigate the impact of PPNs (Vishwakarma et al. 2022). AMF are obligatory root symbionts estimated to colonize more than 80% of land plant species. They improve plant growth through enhanced nutrient uptake in exchange for photosynthetic carbon from the host (Smith et al. 2010; Sameeullah et al. 2016). AMF can also alleviate abiotic and biotic stresses, including damage caused by PPNs (Spagnoletti et al. 2021). In addition to their nutritional benefits, AMF may induce systemic resistance in plants, thereby enhancing defense responses against invading pathogens (Weng et al. 2022).

Similarly, *Trichoderma* spp., a genus of filamentous fungi commonly found in soil, are well known for their biocontrol activity against a wide range of plant pathogens, including PPNs (Hariharan et al. 2022). *Trichoderma* species produce enzymes, antibiotics, and secondary metabolites that can degrade nematode eggs, immobilize juveniles, and suppress reproduction (Lopes et al. 2024). They can also induce systemic resistance through activation of key defense signaling pathways involving salicylic acid (SA), jasmonic acid (JA), and ethylene (ET) (Guzmán-Guzmán et al. 2023). Therefore, the combined use of AMF and *Trichoderma* may provide a stronger and more multifaceted strategy for nematode management than either organism alone.

Endophytic fungi, which reside within plant tissues without causing harm, also contribute to plant growth promotion and biological control (Dababat and Sikora 2007). Several endophytic fungi produce nematocidal metabolites, such as chaetoglobosins and other bioactive compounds, that suppress nematode growth and development (Li et al. 2014; Ashrafi et al. 2023). In addition, these fungi may enhance nutrient uptake and stress tolerance in host plants (Sodhi and Saxena 2023). These findings collectively highlight the potential of beneficial fungi for sustainable management of PPNs.

Despite the documented individual benefits of AMF and *Trichoderma*, their combined effects against cereal cyst nematodes in wheat remain insufficiently understood. In particular, little is known about whether co-application of these beneficial fungi can synergistically improve resistance through coordinated changes in nutrient homeostasis, metabolic defense responses, and gene expression (Fernandez-Gnecco et al. 2024; Ding et al. 2025; Umer et al. 2025). Moreover, integrated studies simultaneously examining ionomic, metabolomic, and transcriptomic responses under CCN stress are lacking. Therefore, the objective of this study was to evaluate the effectiveness of AMF, *Trichoderma*, and their combination against CCN in wheat seedlings by assessing ionomic, metabolomic, and transcriptomic responses.

Materials and Methods

Plant Materials and Growth Conditions

The seeds of wheat (*Triticum aestivum* L., cv. Bezostaya a CCN sensitive) were surface-sterilized and germinated in Petri plates at 22 °C for several days in darkness. Uniform seedlings were then transferred to a sterile soil mixture consisting of 70% sand and 30% silt, and inoculated with either the AMF consortium, *Trichoderma* alone, or a combination of both. This study employed *Trichoderma harzianum* Rifai KRL-AG2 (T-22 Planter Box®; 4×10^8 spores/g) as a biological control agent, together with ERS® (Endo Roots Soluble), a commercial AMF formulation. ERS® contains 87.85 propagules/g and delivers approximately 150 mg of an AMF consortium per plant, comprising spores of *Glomus intraradices*, *G. aggregatum*, *G. mosseae*, *G. clarum*, *G. monosporum*, *G. deserticola*, *G. brasilianum*, *G. etunicatum*, and *Gigaspora margarita* (15 spores/plant). Following inoculation, the seedlings were maintained in a controlled-environment growth room at 20 °C for three weeks to allow the establishment of AMF or *Trichoderma* colonization. Subsequently, 200 s-stage juveniles (J2s) of *H. filipjevi* were inoculated into three small holes created around the root zone using a sterile plastic rod. After nematode inoculation, plants were grown under controlled conditions with a 16/8 h light/dark photoperiod, 65% relative humidity, and a temperature of 24 °C for the remainder of the experiment.

Plants were irrigated with distilled water at 5-day intervals to maintain adequate soil moisture. In addition, a modified half-strength Hoagland nutrient solution (Hoagland and Arnon 1950) containing a reduced phosphate concentration (25 µM KH_2PO_4) was supplied once every two weeks.

The inocula of AMF and *Trichoderma* were applied following the methodology by Zhang et al. (2017a) and Yan et al. (2021).

Scoring of Cereal Cyst Nematodes

Nematodes were assessed following previously described procedures (Renčo et al. 2018). Briefly, the reproduction rate of cereal cyst nematodes (CCN, *H. filipjevi*) was calculated using the equation Rf = Pf / Pi, where Rf denotes the reproduction factor, Pf represents the final nematode population density recorded at the end of the experiment, and Pi corresponds to the initial population density (200 s-stage juveniles, J2) (Oostenbrink, 1966; Pariyar, 2010). *H. filipjevi* individuals were extracted using a modified Baermann funnel technique as described by Hooper (1986). The Rf values were calculated based on nematode counts obtained from plant root samples along with their corresponding soil samples, with six plants per replication and three replications per treatment. Nematode staining in wheat roots was carried out according to the method described by Byrd et al. (1983).

Quantification of Arbuscular Mycorrhizal Fungi and *Trichoderma* Occupancy in Root Systems

AMF and *Trichoderma* root colonization was quantified under a brightfield light microscope (McGONIGLE et al. 1990), using at least 50 intersections per root sample following stained by trypan blue. Staining was performed using six plant roots per replication and three replications per treatment.

Ionomics Analysis

Plants were uprooted one month after treatment and shoots were washed carefully to remove external dust particles. Then excised shoots were dried at room temperature and wet digestion was performed using HNO_3 and H_2O_2. The digested solution was made up to 20 mL and ions were analyzed using ICP-OES, AAS following the procedure as described earlier (Yeken 2023). Three independent biological replicates per treatment were used and each replication was consist of one plant.

Metabolomics Analysis

Plants were harvested one month after treatment. Roots were carefully washed to remove soil particles, gently blotted with paper towels to remove excess moisture, and excised. Root tissues were immediately snap-frozen in liquid nitrogen and stored at − 80 °C until analysis. Metabolites were extracted using 70% methanol following the procedure described by Shi et al. (2021). Extracts were filtered through 0.22 µm membranes prior to LC–MS analysis (El-Sharkawy et al. 2018; Shi et al. 2021). LC–MS analysis was performed using an Agilent 1290 Infinity UHPLC system coupled to an Agilent 6540 Quadrupole Time-of-Flight (Q-TOF) mass spectrometer equipped with a Dual AJS electrospray ionization (ESI) source. Chromatographic separation was achieved on an Agilent Zorbax SB-C18 column (RRHD, 2.1 mm × 100 mm, 1.8 µm) maintained at 60 °C. Mass spectrometric acquisition was conducted in both positive and negative ionization modes (ESI + and ESI−) using full-scan acquisition over the m/z range 100–1,200. Metabolite annotation was performed based on accurate mass, retention time, and MS/MS spectral matching against publicly available metabolite databases including HMDB and METLIN. Metabolomic analyses were performed using three independent biological replicates, with each biological replicate consisting of root tissue from one individual plant per treatment. Metabolite abundance data were normalized and autoscaled prior to multivariate and statistical analyses in MetaboAnalyst 6.0. Statistical significance among treatments was determined using one-way ANOVA followed by Tukey's post-hoc test. False discovery rate (FDR)-adjusted *p*-values were used with a significance threshold of FDR < 0.1.

RNA Isolation

One month after inoculation with CCN and supplementation with AMF, *Trichoderma* alone, or a combination of both, wheat seedlings were carefully uprooted without damaging the roots and gently washed to remove adhering soil particles. Then root tissues were excised with sharp razor and immediately snap frozen in liquid nitrogen and transferred to -80 °C freezer for further processing. The total RNA was isolated using RNeasy Plant Mini Kit (Qiagen) and DNase I was used to remove genomic DNA contamination. The quality of total RNA was measured using nanodrop and also RIN values using Agilent 2100 Bioanalyzer. The high-quality RNA was used for RNA sequencing.

RNA Sequencing

RNA isolated as described above was used for transcriptomic profiling following treatment with AMF, *Trichoderma*, or a

combined AMF + *Trichoderma* inoculation in the presence of CCN, with plants inoculated only with CCN serving as the control. Three independent biological replicates per treatment were used and each replicate consisted of one plant. RNA sequencing was performed using next-generation sequencing to determine gene expression profiles, compare selected groups statistically, and report significantly altered genes, gene ontologies, and pathways. RNA quantity, purity, and integrity were assessed using Qubit 3 Fluorometer (Thermo Fisher, USA, #Q33216) and Agilent 2100 Bioanalyzer (#G2939BA) or 4200 TapeStation (#G2991BA). Libraries were prepared with the Illumina Total RNA Prep kit (#20040529), which includes rRNA depletion, fragmentation, cDNA synthesis, indexing, and purification following the manufacturer's instructions. Sequencing was conducted on the Illumina NovaSeq 6000 platform, targeting ~ 30 million 150 bp paired-end reads per sample. Library preparation and loading followed manufacturer protocols. FASTQC was used for raw read quality control, assessing read quality, GC content, kmer profiles, and adapter contamination. Low-quality bases and adapter/index sequences were trimmed using Trimmomatic v0.39 (Bolger et al. 2014). Cleaned reads were analyzed with the Illumina DRAGEN RNA Pipeline, aligning to the Triticum aestivum IWGSC CS RefSeq v2.1 reference genome, with annotation from the corresponding GTF file. Read counts were normalized to RPK and then TPM. Differential expression analysis used edgeR with the Quasi-Likelihood model (Robinson et al. 2010). Gene ontology enrichment was performed with TopGO using the KS test (Alexa and Rahnenfuhrer 2010), and pathway analysis with clusterProfiler (Yu et al. 2012). R scripts were used for statistical analyses, visualization, and reporting.

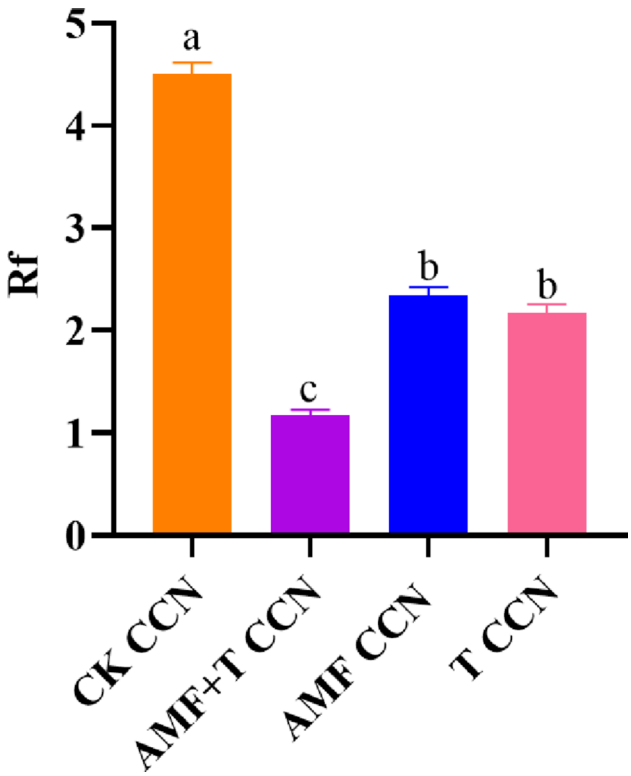


Fig. 1 Reproduction factor (Rf) of cereal cyst nematode (CCN) in the wheat cultivar Bezostaya under Control (CK), *Trichoderma* (T), AMF, and AMF + *Trichoderma* treatments. Data are presented as mean ± SE. Different letters above the bars indicate significant differences among treatments according to one-way ANOVA followed by Tukey's post hoc test ($P < 0.05$)

qRT-PCR

Total RNA extracted from roots of control and treated plants was also used to synthesize cDNA. qRT-PCR was employed to determine the expression level of plant-pathogen interaction (Traes_5BL_E0E3EC75D.1, Traes_5DL_43D95A3FE.1 and Traes_2AL_074F05306.1), plant hormone signal transduction (Traes_3B_2380CD0DB.1), MAPK signaling pathway (Traes_1BL_9DA22ABF9.1) and phenylpropanoid biosynthesis (Traes_7DL_67EAA72F1.1) response genes to determine the cascade of defense response in wheat due to application of AMF and *Trichoderma*. The *TaGPDH* gene was used to normalize the gene expression. To perform this experiment, the procedure was followed as described earlier (Sameeullah et al. 2013, 2021). The primers are listed in Supplementary Table 1. Three independent biological replicates per treatment were used and each replication was consist of one plant.

Results

The CCN population scoring (1.17) indicated that the combined treatment with AMF + *Trichoderma* effectively reduced the CCN population in the sensitive Bezostaya cultivar compared to the control (CK, 4.50) and to treatments where AMF (2.33) or *Trichoderma* (2.17) were applied individually (Fig. 1). The combined AMF + *Trichoderma* treatment most effectively reduced CCN populations compared to individual treatments and the untreated control.

Symbiotic Interactions and Quantification of AMF and *Trichoderma* Colonization

The root colonization percentage of AMF, either alone or in combination with *Trichoderma* reached substantial levels (≥45%). Additionally, colony-forming units (CFUs) of *Trichoderma* (≥4 CFU g^{-1} root) were detected in wheat roots, both in singular and co-inoculation treatments (Fig. 2). The observed levels of AMF colonization and *Trichoderma* CFUs suggest successful establishment of a

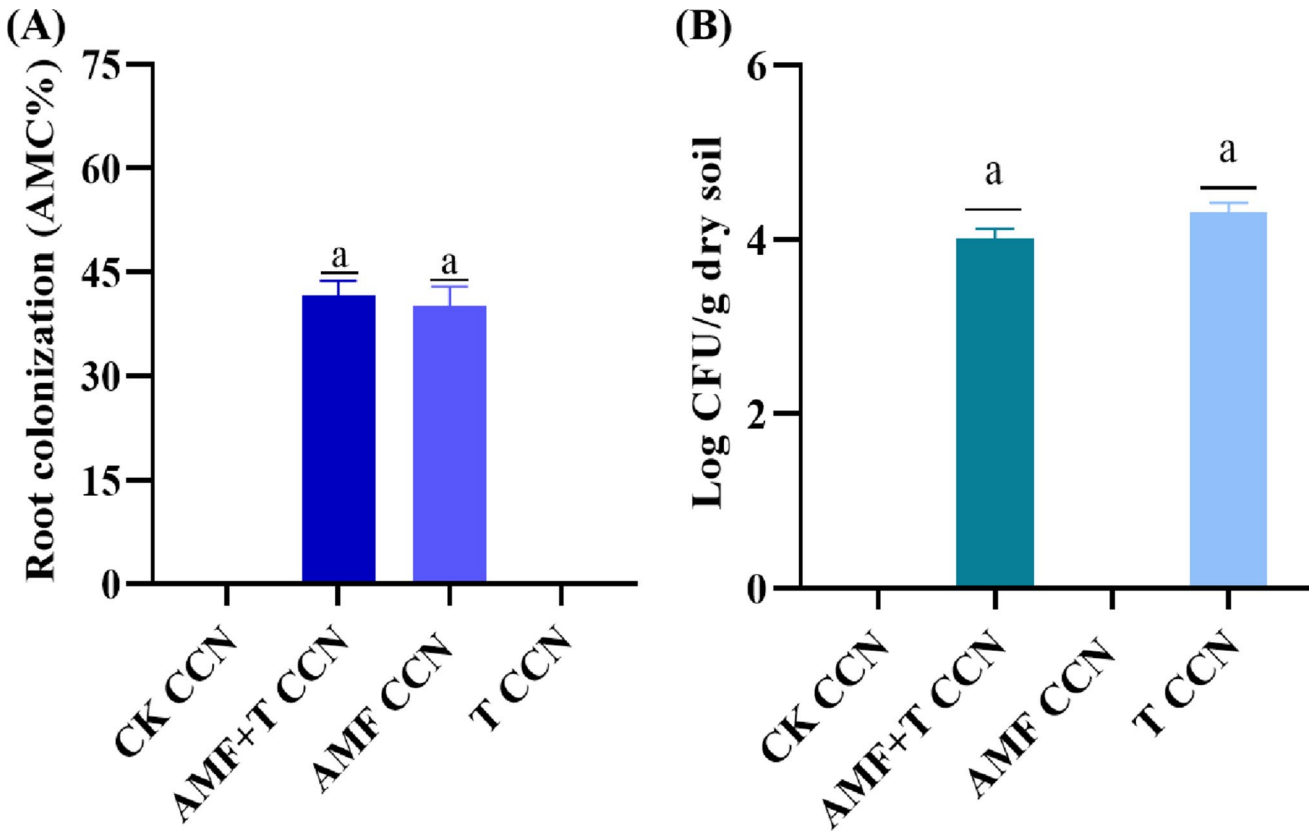


Fig. 2 Root arbuscular mycorrhizal colonization (AMC) (%) in AMF and AMF + *Trichoderma* treatments (**A**), and soil *Trichoderma* colony-forming units (CFU) in *Trichoderma* and AMF + *Trichoderma* treatments (**B**) of wheat plants infected with cereal cyst nematode (CCN). Data are presented as mean ± SE. Different letters above the bars indicate significant differences between treatments according to one-way ANOVA followed by Tukey's post hoc test ($P < 0.05$)

symbiotic relationship in the Bezostaya wheat cultivar, supporting its potential for enhanced biocontrol against CCN.

AMF and *Trichoderma* Impact on Plant Ionomics

A treatment of *Trichoderma* + AMF synergistically and significantly enhanced nitrate (NO_3) levels in wheat shoots (Fig. 3A). While individual treatments of *Trichoderma* and AMF also resulted in NO_3 levels significantly higher than in the control, their effects were less pronounced than the combined treatment. These results suggest that a mixture of *Trichoderma* and AMF can effectively improve NO_3 levels in wheat.

Potassium (K) levels were also significantly enhanced in the mixed treatment compared to individual treatments or the control (CK) (Fig. 3B). Similarly, the levels of the micronutrients iron (Fe) (Fig. 3C), manganese (Mn) (Fig. 3D), and zinc (Zn) (Fig. 3E) were significantly enhanced by the AMF + *Trichoderma* treatment when compared to individual treatments or the control. These results suggest that the combined application can synergistically improve both macro- and micronutrient uptake in wheat plants. Whereas calcium (Ca) content was not significantly different among all treatments (Supplementary Fig. 1A). Magnesium (Mg) content was significantly higher in the CK but not in the individual or combined treatments (Supplementary Fig. 1B). Phosphate (P) content was found to be significantly higher in the mycorrhizal treatment than in the *Trichoderma* (T), combined, or control treatments (Supplementary Fig. 1C). These results suggest that AMF can effectively enhance P content in wheat shoots. Copper (Cu) content was significantly higher in individual treatments of *Trichoderma* or AMF compared to the combined treatment or the CK (Supplementary Fig. 1D). These results suggest that Cu uptake was enhanced by individual microbial applications. The corresponding genes related to NO_3 (TraesCS6B03G0694500), K (TraesCS2A03G0239200), Fe (TraesCS7D03G0222500), Zn (TraesCS6A03G0229000, TraesCS7A03G1017300), and Mn (TraesCS4A03G0096800) were upregulated (Supplementary Dataset S1), thus corroborating their possible function in ion transport and accumulation in wheat plants.

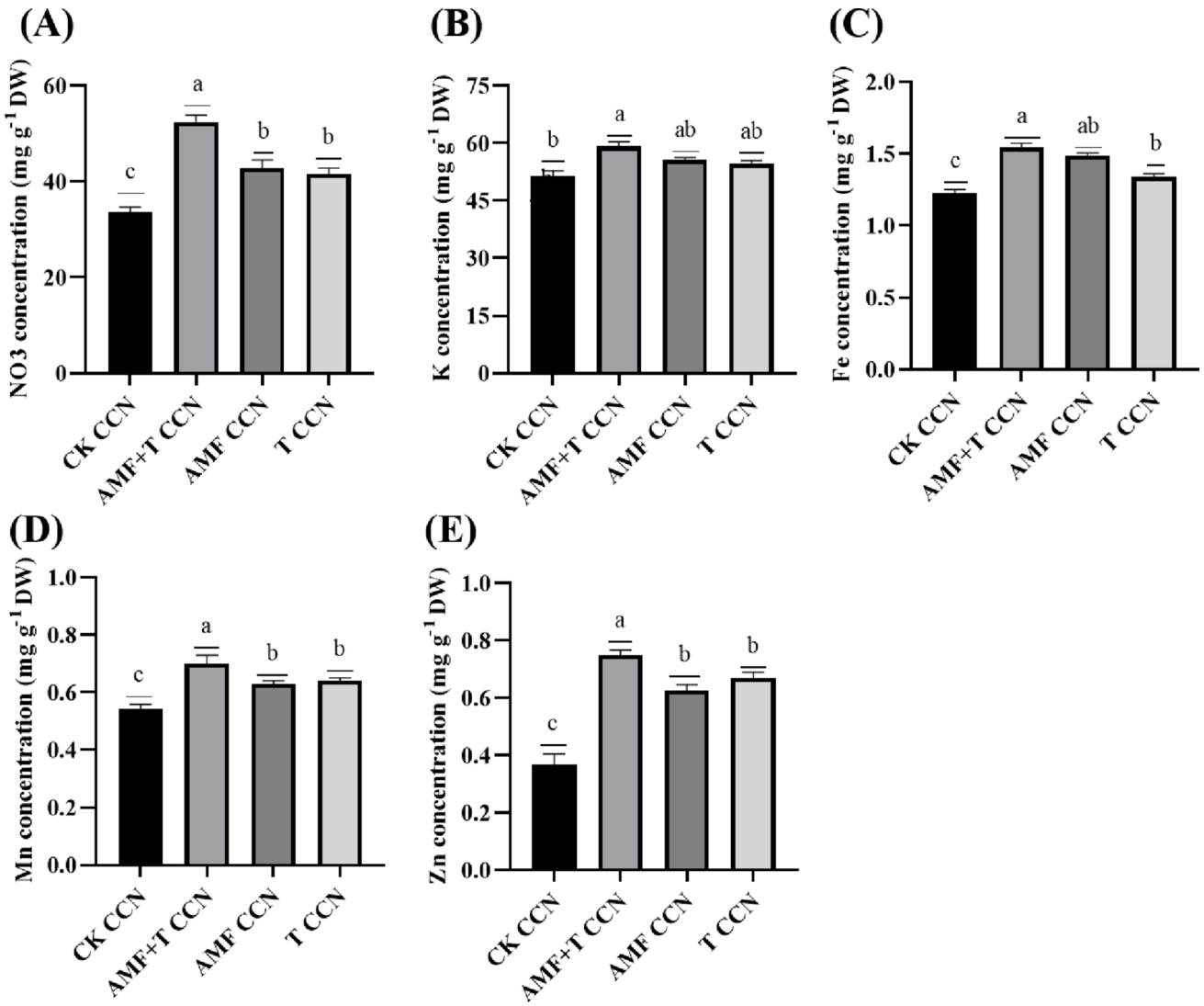


Fig. 3 Effect of *Trichoderma* and arbuscular mycorrhizal fungi (AMF), applied individually or in combination, on the nutrient content of wheat in the presence of cereal cyst nematode (CCN). Concentrations of (**A**) nitrate, (**B**) potassium, (**C**) iron, (**D**) manganese, and (**E**) zinc were determined in Control (CK), *Trichoderma* (T), AMF, and AMF + *Trichoderma* treatments under CCN infestation. Different letters indicate significant differences among treatments according to Fisher's least significant difference (LSD) test following one-way ANOVA ($P < 0.05$)

AMF and *Trichoderma* Impact on Plant Metabolomics

Partial least squares-discriminant analysis (PLS-DA) revealed distinct metabolomic profiles among CK CCN, AMF CCN, T CCN, and AMF + T CCN treatments (Fig. 4). Component 1 and Component 2 accounted for 12.6% and 11.0% of the total variance, respectively. AMF CCN samples formed a tight, well-separated cluster along the negative axis of Component 1, while CK CCN samples clustered in the central-to-positive region of Component 1. AMF + T CCN samples occupied an intermediate position with moderate separation from CK CCN, whereas T CCN samples showed broader dispersion along Component 1, reflecting greater within-group variability. These distinct clustering patterns indicate that microbial inoculation induced systematic shifts in metabolite profiles under CCN stress.

Hierarchical clustering heatmap analysis further resolved distinct metabolite accumulation patterns across all four treatment groups (Fig. 5). Samples clustered into four color-coded groups consistent with treatment identity, confirming reproducible metabolomic differences among replicates. Amino acids including L-arginine, tryptophan, and lysine, as well as secondary metabolites such as trans-cinnamic acid derivatives, kauralexin A2, and 2-descarboxy-betanidin, displayed notably elevated accumulation in AMF CCN and T CCN treatments relative to CK CCN plants. By contrast, N-(3-acetamidopropyl)-4-aminobutanal and

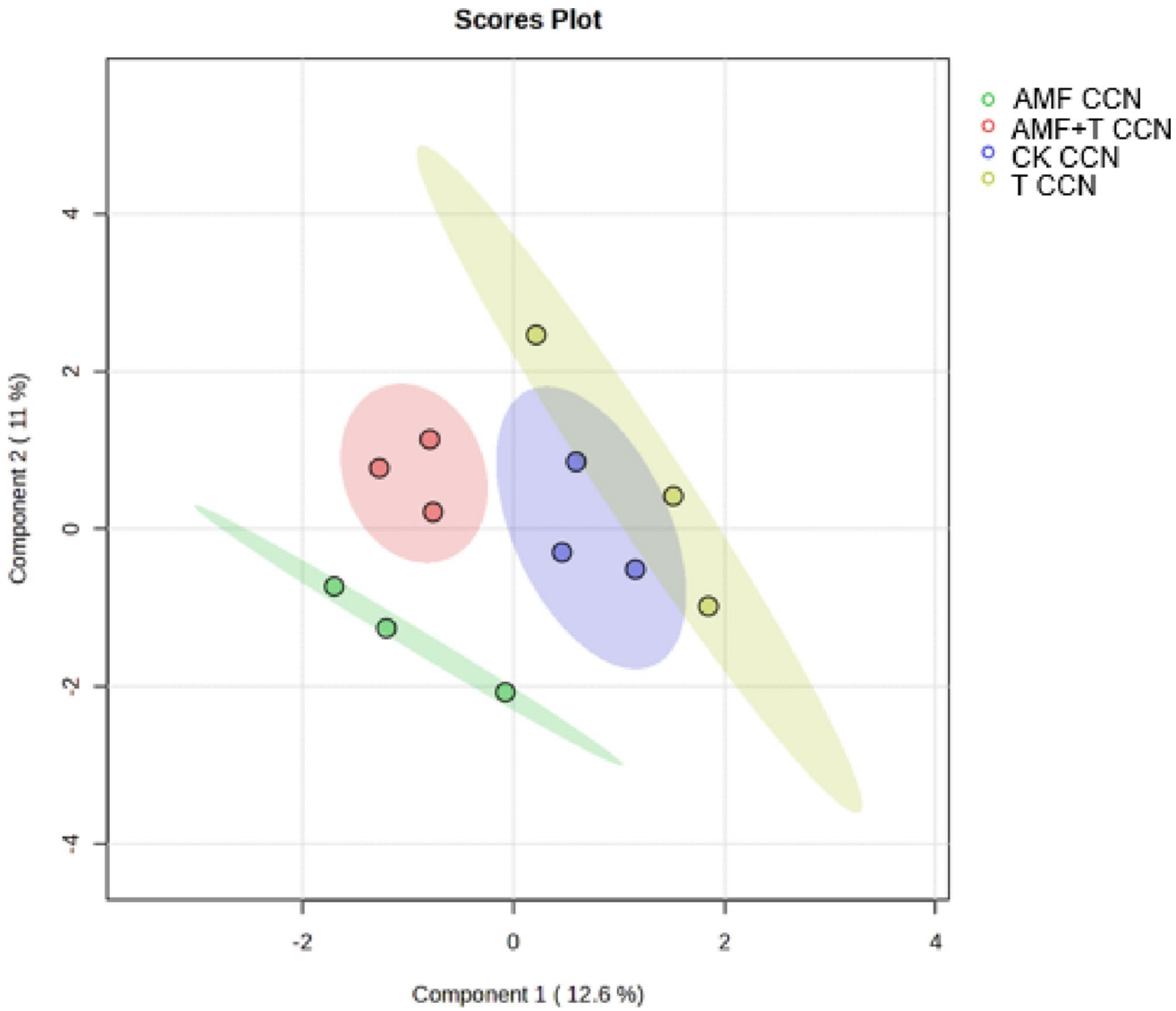


Fig. 4 Partial least squares-discriminant analysis (PLS-DA) score plot showing metabolomic variation among AMF CCN, AMF + T CCN, CK CCN, and T CCN treatments under cereal cyst nematode stress. Component 1 and Component 2 explained 12.6% and 11.0% of the total variance, respectively. Each point represents an individual biological replicate ($n = 3$), and shaded ellipses indicate group clustering patterns based on metabolite profiles

cinnamoyltyramine showed higher relative abundance in CK CCN samples. AMF + T CCN-treated plants exhibited metabolite profiles distinct from CK CCN plants, though with some similarities to T CCN samples in secondary metabolite clusters.

Variable importance in projection (VIP) analysis identified 15 metabolites contributing to group discrimination, with VIP scores ranging from near zero to approximately 1.9 (Fig. 6). N-(3-acetamidopropyl)-4-aminobutanal exhibited the highest VIP score (~ 1.9), followed by L-arginine (~ 1.7), kauralexin A2 (~ 1.5), cis-aconitate (~ 1.5), and tryptophan (~ 1.35). Metabolites with moderate VIP scores (> 0.8) included D-aspartic acid and N-alpha-methyl-L-histidine, while phytosphingosine, lysine, and 2-descarboxy-betanidin showed intermediate contributions (VIP 0.4–0.7). Indole-3-acetyl derivatives, cinnamoyltyramine, deoxypumiloside, 1,3,7-trimethyl-5-oxo derivatives, and trans-cinnamic acid-related compounds contributed less to group separation (VIP < 0.2). The associated concentration heatmap indicated that AMF CCN and AMF + T CCN treatments generally had higher relative abundances of N-(3-acetamidopropyl)-4-aminobutanal and L-arginine compared with CK CCN and T CCN plants.

One-way ANOVA followed by Tukey's post-hoc test identified two metabolites exhibiting significant treatment-dependent variation among CK CCN, AMF CCN, T CCN, and AMF + T CCN groups (Fig. 7). The relative normalized abundance of 2-descarboxy-betanidin was markedly

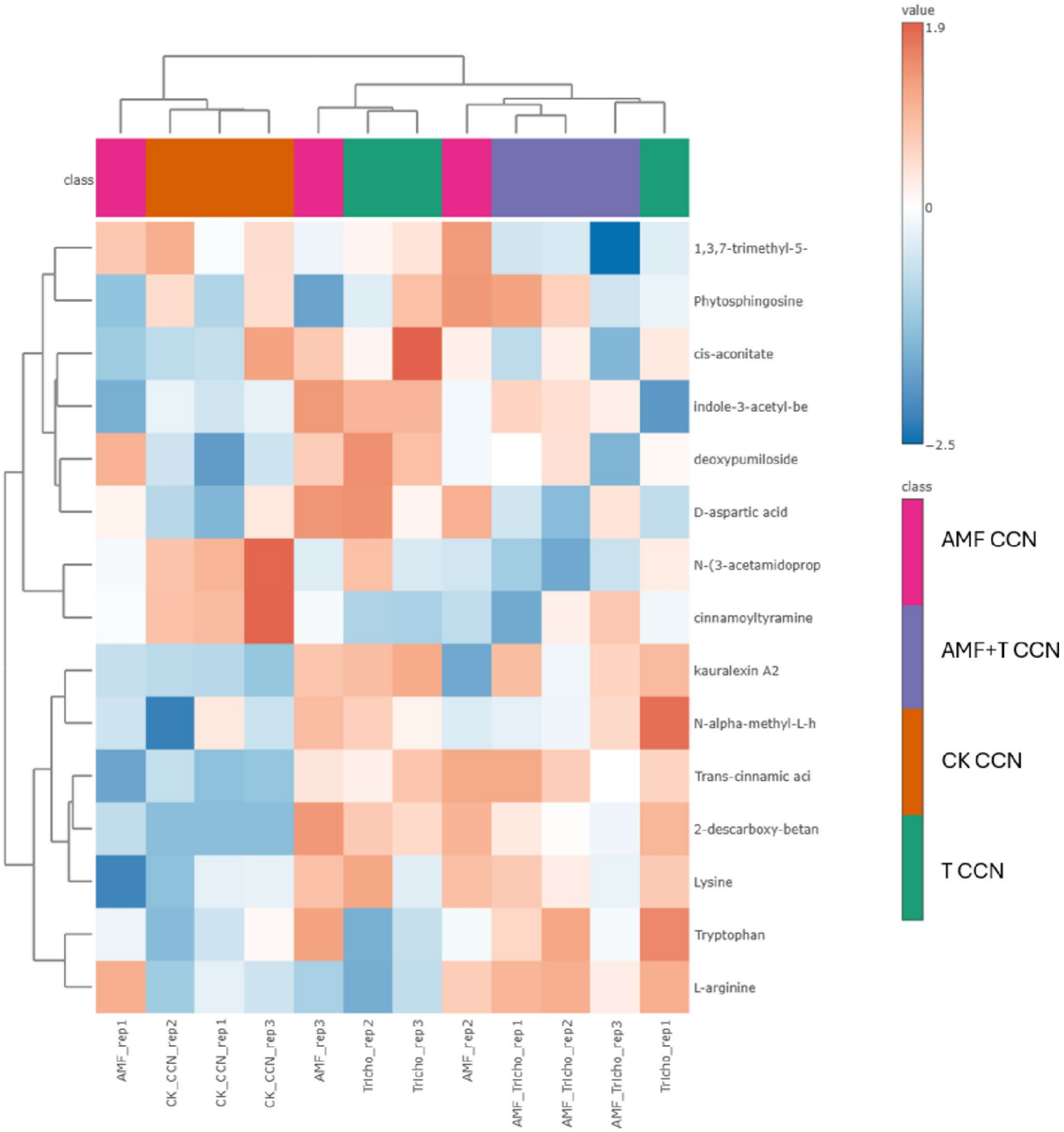


Fig. 5 Hierarchical clustering heatmap of metabolite profiles in wheat roots under cereal cyst nematode (CCN) stress. Rows represent metabolites, and columns represent biological replicates from AMF CCN, AMF + T CCN, CK CCN, and T CCN treatments. Red and blue indicate relatively high and low metabolite abundance, respectively. AMF, arbuscular mycorrhizal fungi; T, *Trichoderma*

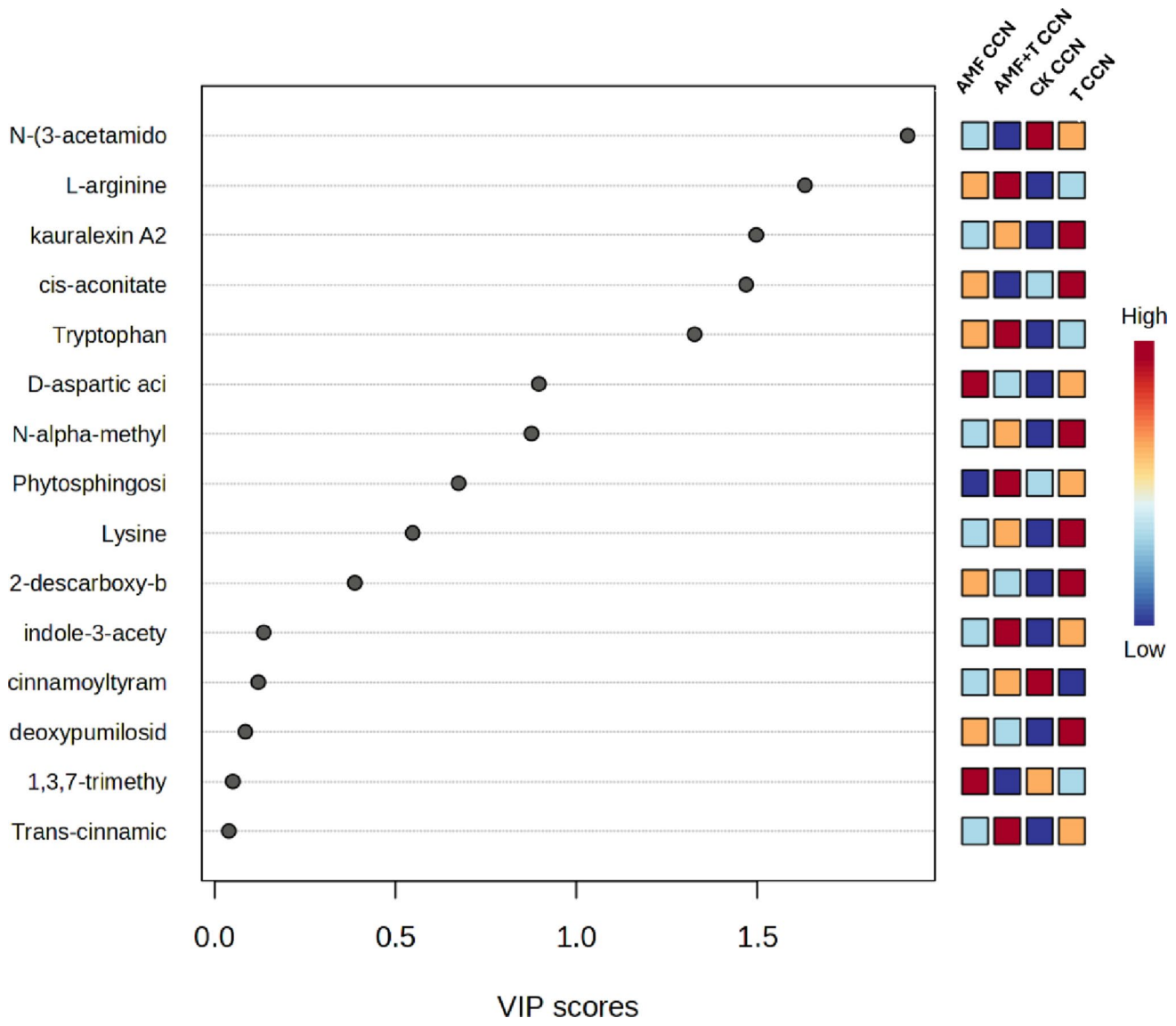


Fig. 6 Variable importance in projection (VIP) scores of metabolites contributing to treatment discrimination among AMF CCN, AMF + T CCN, CK CCN, and T CCN groups based on PLS-DA. Colored boxes indicate relative metabolite abundance across treatments (red = high, blue = low). AMF, arbuscular mycorrhizal fungi; T, *Trichoderma*

lower in CK CCN plants, whereas the highest abundance was observed in AMF + T CCN plants, followed by T CCN and AMF CCN treatments (Fig. 7A). In contrast, N-(3-acetamidopropyl)-4-aminobutanal exhibited the highest abundance in CK CCN plants and the lowest abundance in AMF + T CCN plants. AMF CCN plants also showed reduced levels of this metabolite, whereas T CCN plants displayed intermediate abundance (Fig. 7B).

AMF and *Trichoderma* Impact on Plant Transcriptome

RNA sequencing of eight samples representing four treatment groups was performed. Sequencing statistics, including read counts, alignment rates, and quality metrics, are presented in Supplementary Table 4. Following filtering of lowly expressed genes and normalization of expression values, all downstream analyses were conducted using normalized data (Supplementary Fig. 2). Principal component analysis (PCA) based on the 500 most variable genes revealed distinct clustering patterns among treatments (Supplementary Fig. 3), indicating treatment-associated differences in global gene expression profiles. Differential expression analysis identified 23,350 genes in the AMF + *Trichoderma* treatment relative to the control. Among these, 1,110 genes were significantly upregulated and 1,718 genes were significantly downregulated (FDR < 0.05), whereas 21,143 genes were not significantly regulated (Fig. 8). The most

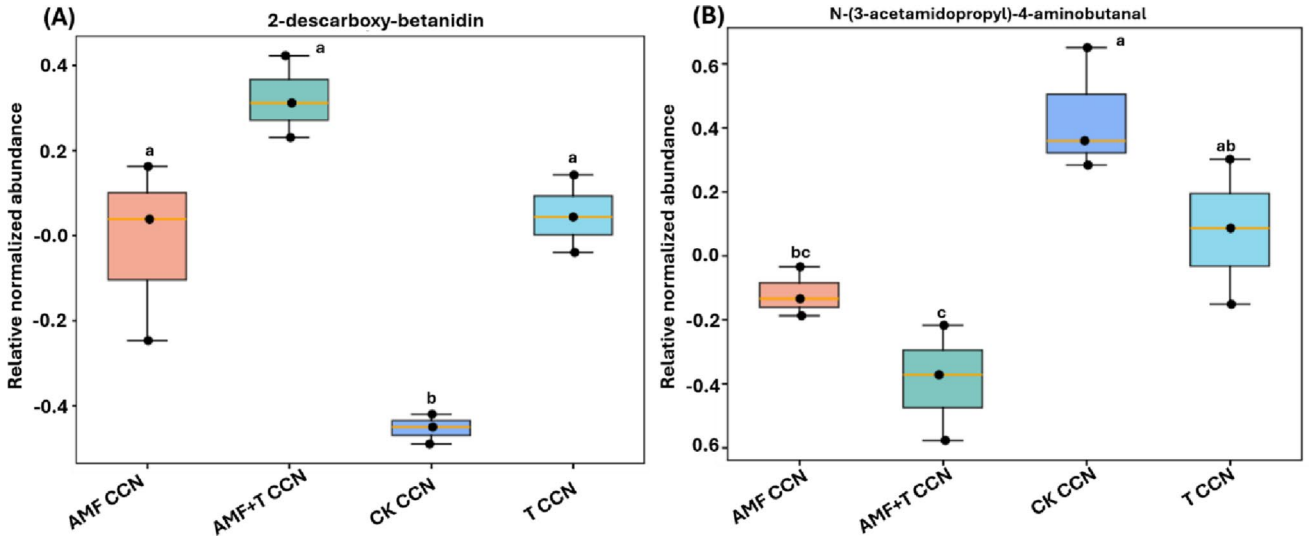
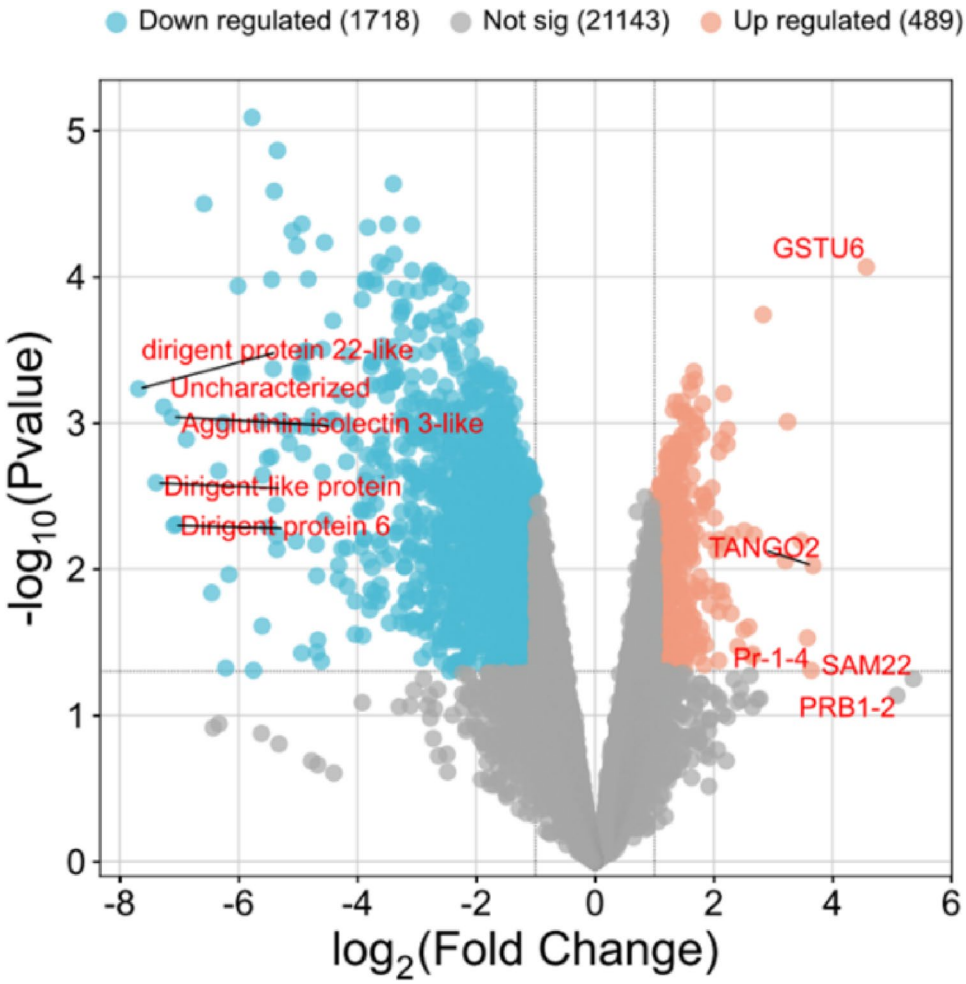


Fig. 7 Relative normalized abundance of selected metabolites across treatment groups under CCN stress. Box plots showing the relative normalized abundance of (**A**) 2-descarboxy-betanidin and (**B**) N-(3-acetamidopropyl)-4-aminobutanal across four treatment groups: AMF CCN, AMF + T CCN, CK CCN, and T CCN. Each box represents the interquartile range (IQR; 25th − 75th percentiles), the orange horizontal line indicates the median, and the black dot indicates the mean. Whiskers represent the minimum and maximum values, and black circles indicate individual biological replicates

Fig. 8 Volcano representation of the genes with the most significant variability



highly upregulated genes included *GSTU6*, *TANGO2*, *PR-1-4*, *SAM22*, and *PRB1-2*, whereas *dirigent protein 22-like*, uncharacterized protein, *agglutinin isolation 3-like*, *dirigent-like protein*, and *dirigent protein 6* were among the most downregulated genes.

Gene Ontology and KEGG Pathway Enrichment Analysis of Upregulated Genes

Gene Ontology (GO) and KEGG pathway enrichment analyses of upregulated genes identified significant enrichment of glutathione metabolism, MAPK signaling pathway–plant, plant hormone signal transduction, glycosphingolipid biosynthesis, arginine biosynthesis, and plant–pathogen interaction pathways (Supplementary Fig. 4)). Glutathione metabolism, MAPK signaling pathway–plant, and plant hormone signal transduction each contained 22–33 enriched genes. The plant–pathogen interaction pathway contained approximately 13 enriched genes, whereas arginine biosynthesis and glycosphingolipid biosynthesis contained 8 and 4 enriched genes, respectively. Sixteen enriched pathways formed five interconnected clusters, while four pathways remained independent (Supplementary Fig. 5). Enriched genes were distributed across all wheat chromosomes, with a higher representation on chromosomes 4B, 1 A, 1D, 1B, 4 A, 6B, 5 A, 3D, 7D, 5B, and 2D (Supplementary Fig. 6; Supplementary Dataset S2).

Enrichment analysis of downregulated genes identified pathways related to linoleic acid metabolism, phenylpropanoid biosynthesis, biosynthesis of various secondary metabolites, cyanoamino acid metabolism, starch and sucrose metabolism, and general metabolic pathways (Supplementary Fig. 7; Supplementary Dataset S3). The chromosomal distribution of downregulated genes is presented in Supplementary Fig. 8. The heatmap in Fig. 9 displays the expression profiles of the 50 most variable protein-coding genes across treatments. Hierarchical clustering separated samples according to treatment and highlighted treatment-specific expression patterns. Among the genes displayed, *PRB1-2* (LOC100873095; Traes_5BL_E0E3EC75D) exhibited the highest expression level in the AMF + *Trichoderma* treatment relative to the other treatments (Fig. 9).

AMF and *Trichoderma* Interaction, and CCN Infection, Modulate Genes Involved in Plant-pathogen Interaction, Hormone Signaling, MAPK Pathway, and Phenylpropanoid Biosynthesis

The expression level of *PRB1-2* was significantly higher in the AMF + T CCN treatment than in CK CCN plants (Fig. 10A). Similarly, *PRB1-3* exhibited significantly increased transcript abundance in AMF + T CCN plants relative to CK CCN plants (Fig. 10B). The expression of *RPM1* was also significantly elevated in AMF + T CCN plants compared with CK CCN plants (Fig. 10C). Likewise, the *BTB* domain-containing protein gene showed significantly higher expression in AMF + T CCN plants than in CK CCN plants (Fig. 10D). The expression level of the *MAPK* kinase substrate protein gene was significantly increased in AMF + T CCN plants relative to CK CCN plants (Fig. 10E). In addition, the *cinnamoyl-CoA reductase 1-like* gene exhibited significantly higher transcript abundance in AMF + T CCN plants than in CK CCN plants (Fig. 10F).

Genomic analysis indicated that *PRB1-2* is located on chromosome 5B, long arm (Supplementary Fig. 9A). Gene structure analysis revealed the presence of 5′ and 3′ untranslated regions (UTRs) and an intronless coding sequence (Supplementary Fig. 9B).

Cis Acting Elements of the *PRB1-2* Gene

Promoter analysis of the *PRB1-2* gene identified several cis-regulatory elements associated with symbiosis, stress responses, and plant defense (Table 1). The OSE1ROOTNODULE motif (AAAGAT), located at positions 333 and 681 on the negative strand, was detected in the promoter region. In addition, two WBOXATNPR1 motifs (TTGAC) were identified at positions 448 on the positive strand and 748 on the negative strand. Eight WRKY71OS motifs (TGAC) were also present throughout the promoter sequence. Furthermore, BOXLCOREDCPAL motifs (ACCWWCC) were identified at positions 91 and 1213, while a WBOXNTCHN48 motif (CTGACY) was detected at position 1336 on the positive strand. These motifs have previously been reported as cis-elements associated with symbiosis-, stress-, and pathogen-responsive transcriptional regulation. Consistent with these findings, genes associated with plant–pathogen interaction pathways were identified among the enriched pathways in the transcriptome dataset (Supplementary Fig. 10).

Subcellular Localization of PRB1-2 Protein

Subcellular localization prediction indicated that PRB1-2 is an extracellular protein localized to the apoplast (Supplementary Fig. 11). No localization signals associated with intracellular organelles, including the nucleus, chloroplast, mitochondrion, or endoplasmic reticulum, were detected.

Protein-protein Interaction

Protein–protein interaction analysis revealed that PRB1-2 was associated with a network of proteins involved in defense- and stress-related functions (Supplementary

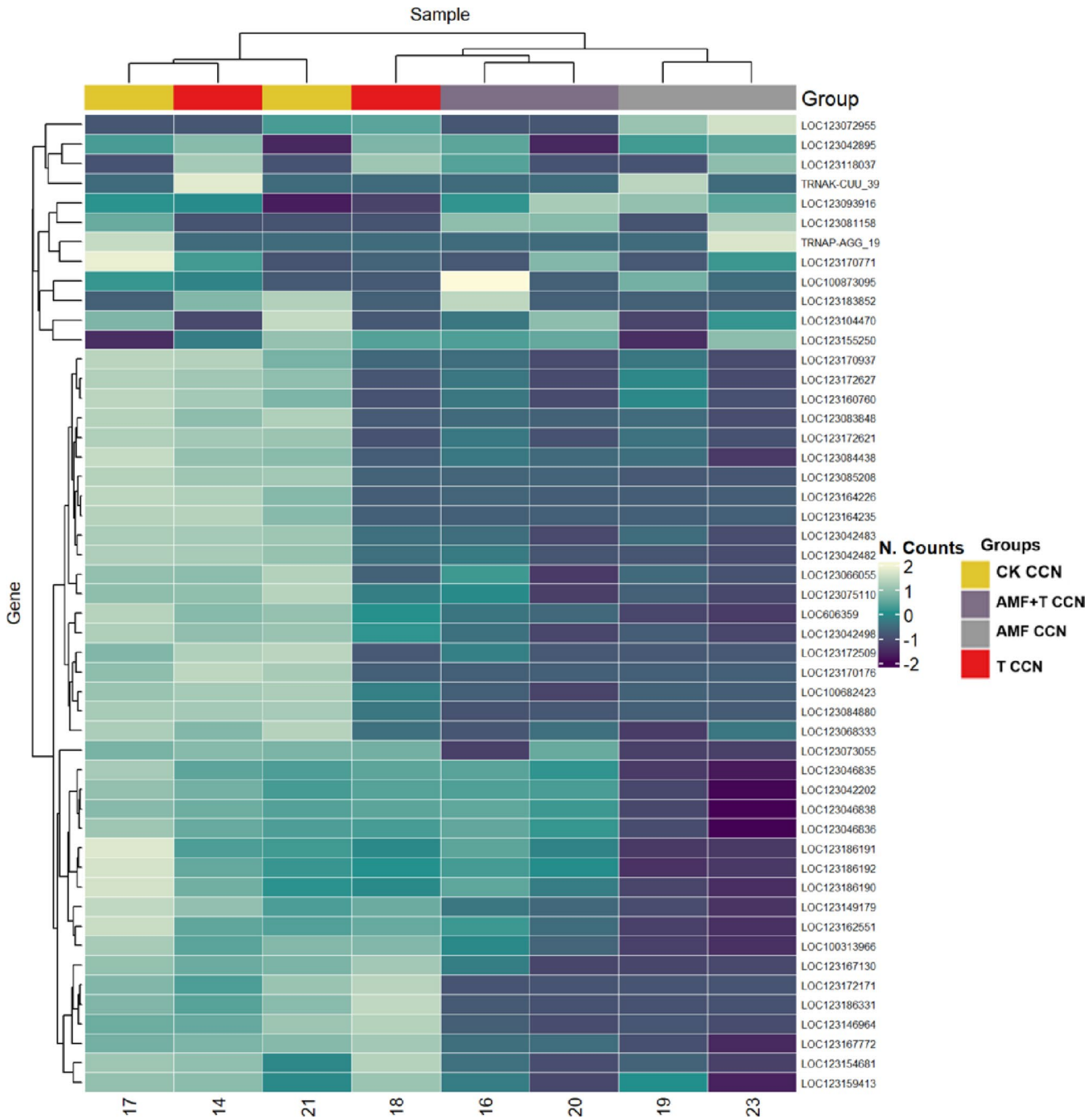


Fig. 9 Expression profile of the top 50 genes showing the greatest variation among samples. Control (CK CCN), AMF + T CCN, AMF CCN, and *Trichoderma* (T CCN) treatments were evaluated in the presence of cereal cyst nematode (CCN; *Heterodera filipjevi*). The dotted rectangle highlights *PRB1-2*, the gene most highly expressed in the AMF + T CCN treatment. AMF, arbuscular mycorrhizal fungi; T, *Trichoderma*

Fig. 12). The interaction network included proteins associated with salicylic acid-responsive pathways, reactive oxygen species-related processes, and chitinase proteins. Several proteins showed direct or indirect interactions with PRB1-2, indicating its integration within a broader protein interaction network. KEGG pathway mapping indicated that PR-1 family proteins, including PRB1-2, were associated with plant–pathogen interaction and salicylic acid-related signaling pathways (Fig. 11). In addition, phenylalanine ammonia-lyase (PAL) was identified as a component of the phenylalanine metabolism pathway connected to the same network (Fig. 11).

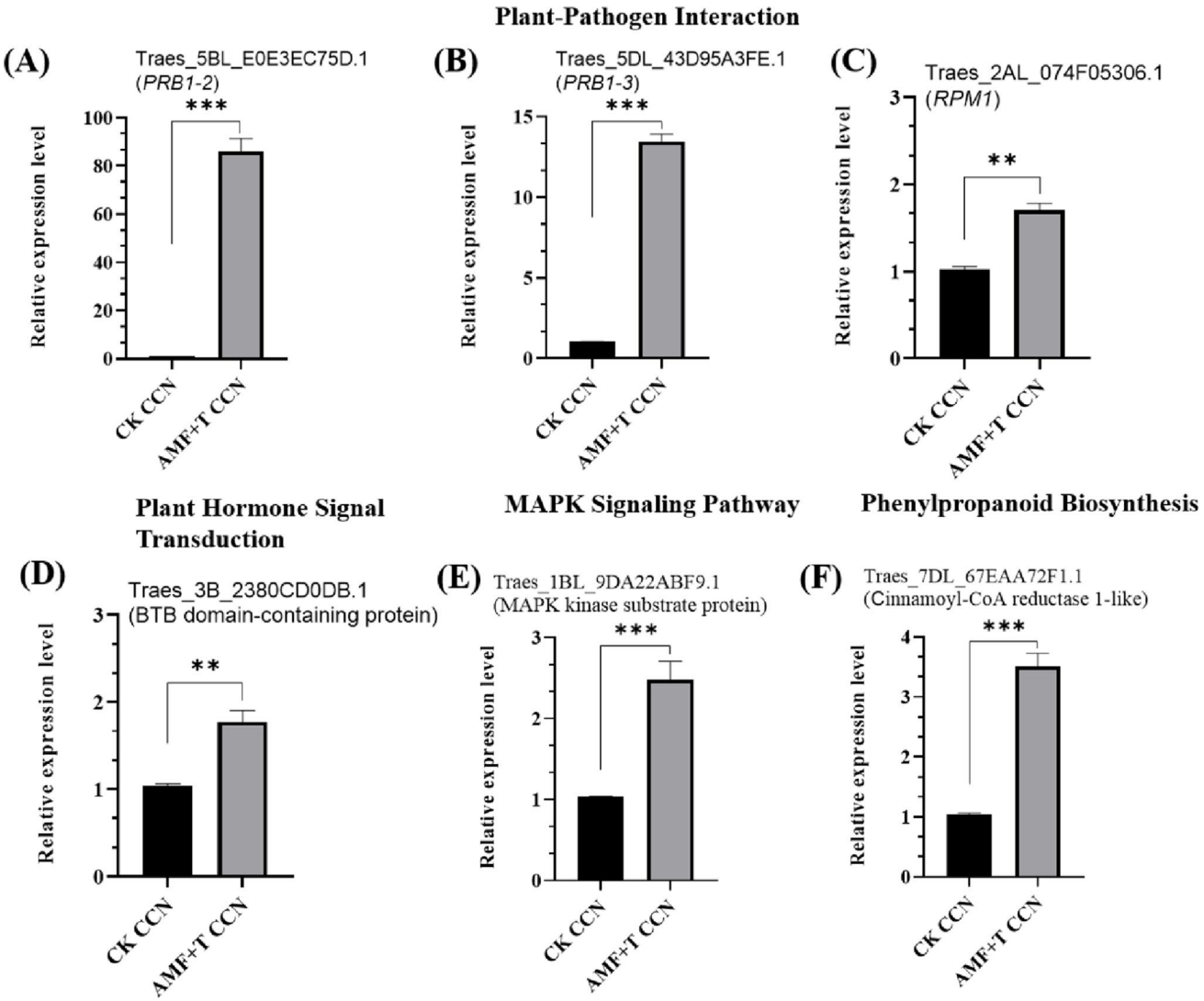


Fig. 10 Relative expression levels of selected genes in wheat under cereal cyst nematode (CCN) stress. Bar graphs show the relative expression levels of selected genes in wheat under CK CCN and AMF + T CCN treatments. Data are presented as mean ± SE. Asterisks indicate significant differences between treatments (**$P < 0.01$; ***$P < 0.001$) based on a two-tailed Student's t-test. AMF, arbuscular mycorrhizal fungi; T, *Trichoderma*

Discussion

CCN Suppression by AMF and *Trichoderma*

The application of AMF + *Trichoderma* reduced CCN populations in the susceptible wheat cultivar Bezostaya more effectively than either agent alone, indicating a synergistic interaction. This is consistent with findings in tomato, where co-inoculation of AMF and *Trichoderma* outperformed individual applications in suppressing *Meloidogyne javanica* (Covacevich et al. 2025). While *Trichoderma* has been documented to control CCN in wheat (Zhang et al. 2014, 2017a; Wang et al. 2024b), and AMF has been shown to suppress other PPN (Schouteden et al. 2015), the present study is among the first to demonstrate their combined efficacy specifically against CCN. The synergism observed likely reflects complementary mechanisms operating sequentially. AMF and *Trichoderma* colonization enhances nutrient uptake, activates metabolic defense pathways, and drives transcriptomic reprogramming, suggesting activation of *PR1*-mediated systemic resistance against CCN.

Effects on Ionomics and Metabolomics

Ionomic analysis revealed that the AMF + *Trichoderma* combination elevated shoot concentrations of NO_3^-, K, Fe, Mn, and Zn under CCN stress, consistent with earlier reports (Moreno-Lora et al. 2023; Bibi et al. 2024; Gao and Zhang 2025; Han et al. 2025). This nutritional enhancement likely constitutes the first mechanistic step underpinning

Table 1 Promoter analysis of the *PRB1-2* gene

Element Name	Position	Strand	Sequence	ID	Function / Expression Induction
OSE1ROOTNODULE	333	(−)	AAAGAT	S000467	Expression due to arbuscules
OSE1ROOTNODULE	681	(−)	AAAGAT	S000467	Expression due to arbuscules
AGMOTIFNTMYB2	1324	(+)	AGATCCAA	S000444	Induced by wounding or elicitor
BOXLCOREDCPAL	1213	(+)	ACCWWCC	S000492	Elicitor response
BOXLCOREDCPAL	91	(−)	ACCWWCC	S000492	Elicitor response
WBOXNTCHN48	1336	(+)	CTGACY	S000508	Elicitor response
ASF1MOTIFCAMV	1080	(+)	TGACG	S000024	Abiotic and biotic stress response
WBOXATNPR1	448	(+)	TTGAC	S000390	Pathogen response
WBOXATNPR1	748	(−)	TTGAC	S000390	Pathogen response
WRKY71OS	268	(+)	TGAC	S000447	Pathogenesis related
WRKY71OS	436	(+)	TGAC	S000447	Pathogenesis related
WRKY71OS	449	(+)	TGAC	S000447	Pathogenesis related
WRKY71OS	666	(−)	TGAC	S000447	Pathogenesis related
WRKY71OS	748	(−)	TGAC	S000447	Pathogenesis related
WRKY71OS	900	(−)	TGAC	S000447	Pathogenesis related
WRKY71OS	965	(+)	TGAC	S000447	Pathogenesis related
WRKY71OS	1080	(+)	TGAC	S000447	Pathogenesis related
WRKY71OS	1337	(+)	TGAC	S000447	Pathogenesis related
NRRBNEXTA	1453	(−)	TAGTGGAT	S000242	Wounding response
WBOXNTERF3	268	(+)	TGACY	S000457	Wounding response
WBOXNTERF3	436	(+)	TGACY	S000457	Wounding response
WBOXNTERF3	899	(−)	TGACY	S000457	Wounding response
WBOXNTERF3	965	(+)	TGACY	S000457	Wounding response
WBOXNTERF3	1337	(+)	TGACY	S000457	Wounding response

reduced CCN establishment, as nutrient-deficient plants exhibit greater susceptibility to nematode damage (Alamri et al. 2022; Wang et al. 2024a).

Downstream of nutritional priming, ANOVA-based statistical analysis of metabolomic data identified two metabolites with significant treatment-dependent variation. 2-descarboxy-betanidin was markedly elevated in AMF + *Trichoderma*-treated plants relative to the untreated control, while N-(3-acetamidopropyl)-4-aminobutanal showed the opposite pattern — highest in the susceptible control and lowest under combined treatment. These contrasting profiles carry distinct mechanistic significance. 2-descarboxy-betanidin is a betalain-related compound with established antioxidant and ROS-scavenging capacity, and its accumulation is consistent with active oxidative defense deployment under nematode challenge (Zeng and Yao 2022). Its elevation aligns with the protein interaction network identified for PRB1-2, which includes ROS-detoxifying enzymes, suggesting a coordinated antioxidant-defense axis activated by the microbial consortium.

The reduction of N-(3-acetamidopropyl)-4-aminobutanal is equally informative. This compound is a terminal catabolite of spermine and spermidine degradation. During compatible cyst nematode interactions, nematode effectors have been shown to manipulate host polyamine catabolism, redirecting spermine pools into such catabolites and thereby depleting a key endogenous inducer of PR proteins (Alcázar et al. 2010; Graska et al. 2023). The marked decrease of this catabolite in AMF + *Trichoderma*-primed plants therefore suggests that biological control agents suppress nematode-driven exploitation of the polyamine pathway, conserving spermine pools available for *PR* gene induction and SA-mediated systemic resistance. This directly connects to the strong transcriptional induction of *PRB1-2* observed in the same treatment, and is consistent with the *NPR1*-mediated SA signaling (Kumar et al. 2022) pathway illustrated in Fig. 11. Taken together, the two statistically significant metabolites tell a coherent resistance story: active antioxidant deployment combined with protection of polyamine-dependent PR gene induction, both converging on SA-mediated CCN suppression.

Supporting these primary findings, VIP analysis further identified shifts in amino acids (arginine, tryptophan, lysine) and secondary metabolites (trans-cinnamic acid derivatives, kauralexin A2), consistent with enhanced nitrogen assimilation and activation of phenylpropanoid and terpenoid defense pathways (Dixon et al. 2002; Schmelz et al. 2014; Sun et al. 2023). Reductions in cinnamoyltyramine and cis-aconitate likely reflect strategic metabolic reallocation toward frontline defense responses. Collectively, these shifts demonstrate that nutritional priming by AMF and *Trichoderma* initiates a cascade of metabolic changes that prime the plant against CCN challenge and feed directly into the transcriptomic reprogramming described below.

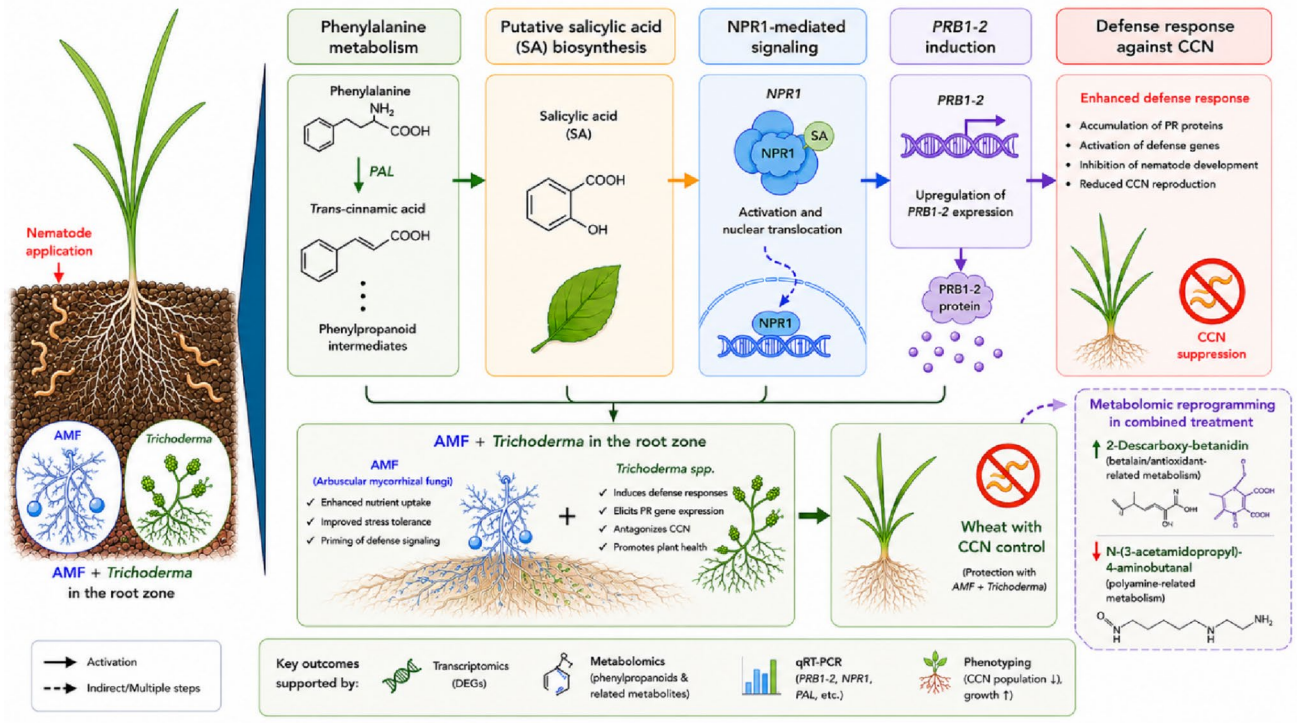


Fig. 11 Proposed model of AMF- and *Trichoderma*-mediated defense signaling against cereal cyst nematode (CCN) in wheat. Root colonization by arbuscular mycorrhizal fungi (AMF) and Trichoderma is associated with alterations in phenylalanine metabolism and defense-related metabolic pathways, including changes in betalain- and polyamine-related metabolites. These responses may contribute to salicylic acid (SA)-associated *NPR1*-mediated signaling, leading to the induction of *PRB1-2* and other defense-related genes. The resulting accumulation of pathogenesis-related proteins and activation of defense responses may contribute to the suppression of CCN development and enhanced resistance in wheat. The proposed model is based on transcriptomic, metabolomic, qRT-PCR, and phenotypic analyses conducted in the present study

Transcriptomic Responses and Defense Gene Activation

Building on this metabolic groundwork, RNA-seq analysis revealed extensive transcriptional reprogramming in the AMF + *Trichoderma* CCN treatment, with over 1,100 genes upregulated and 1,700 downregulated relative to the untreated control. KEGG pathway enrichment confirmed activation of glutathione metabolism, *MAPK* signaling, plant hormone signal transduction, and plant-pathogen interaction pathways, all central to biotic stress responses (Tsuda and Katagiri 2010; Meng and Zhang 2013). The MAPK cascade, activated early upon pathogen recognition, serves as a critical signal relay connecting upstream perception events to downstream transcriptional reprogramming, including defense gene induction (Cristina Rodriguez et al. 2010). Upregulation of genes in glycosphingolipid biosynthesis and arginine metabolism is consistent with the metabolomic findings described above, supporting a coherent cross-layer defense response (Cacas et al. 2015; Graska et al. 2023).

Among the most strongly upregulated defense genes were *PRB1-2*, *PRB1-3*, *RPM1*, *BTB* domain-containing protein, *MAPK* kinase substrate protein, and *Cinnamoyl-CoA reductase 1*-like. The induction of *RPM1*, a canonical *R* gene, indicates engagement of effector-triggered immunity (ETI) as part of the broader transcriptional defense response (Dodds and Rathjen 2010). Notably, SA-dependent pathways dominated the transcriptomic response, while jasmonic acid (JA)-related genes were not significantly upregulated. This pattern is consistent with the established dominance of SA signaling in defense against biotrophic pathogens such as cyst nematodes, in contrast to JA, which predominantly mediates resistance to necrotrophic pathogens and herbivores (Glazebrook 2005). The downregulation of phenylpropanoid biosynthesis and starch/sucrose metabolism genes likely reflects a temporal reallocation of resources toward acute defense responses during the early phase of nematode challenge (Naoumkina et al. 2010).

In silico Functional Insights into *PRB1-2*

PRB1-2 emerged as the most prominently upregulated gene and was selected for in silico functional analysis. PR1-family proteins are particularly relevant in cyst nematode resistance, as SA-mediated systemic acquired resistance

has been shown to restrict nematode establishment and reproduction by priming the plant immune system prior to and during infection (Durrant and Dong 2004; van Loon et al. 2006). As a member of this family, *PRB1-2* serves as a canonical marker of SA-mediated SAR. The strong transcriptional induction of *PRB1-2* observed in RNA-seq data is supported by its promoter architecture, where analysis identified cis-regulatory elements including WBOXATNPR1, WRKY71OS, and OSE1ROOTNODULE, which are recognized binding sites for WRKY transcription factors activated downstream of SA signaling and during mycorrhizal symbiosis (Lebel et al. 1998; Hussain et al. 2018). These promoter elements suggest that AMF + *Trichoderma* colonization drives PRB1-2 induction through SA-dependent WRKY-mediated transcription under dual microbial and nematode challenge. In silico localization prediction indicates that *PRB1-2* resides in the apoplast, consistent with a role in restricting pathogen ingress at the plant–nematode interface (Sels et al. 2008), while protein interaction network analysis identified *PRB1-2* as a hub connecting chitinases and ROS-detoxifying enzymes, reinforcing its integration into the broader SA-mediated defense network. Taken together, the promoter, expression, localization, and interaction data converge to position *PRB1-2* as a strong candidate gene for future functional validation and nematode-resistance breeding. Future studies should focus on functional validation of *PRB1-2* through CRISPR-based genome editing approaches, including gene activation via promoter targeting and gene silencing or knockout, alongside promoter functional analyses, to confirm its putative role in SA-mediated resistance against CCN in wheat. Complementary approaches, including hormone profiling, protein localization, nematode infection assays, and protein–protein interaction studies, will further elucidate the molecular mechanisms and regulatory networks associated with *PRB1-2*-mediated defense.

Implications for Sustainable Wheat Management

The mechanistic cascade described above, spanning microbial colonization and nutrient enhancement, through metabolic defense priming, to SA-mediated transcriptional reprogramming and putative PR1-mediated resistance, collectively explains the significant reduction in CCN populations observed under combined AMF + *Trichoderma* treatment. The dominance of SA-mediated over JA-mediated responses indicates a specialized immune strategy tailored to biotrophic nematode attack. These results support the deployment of the AMF–*Trichoderma* consortium as eco-friendly biocontrol agents within integrated nematode management programs, with particular relevance to sustainable wheat production systems where chemical nematicides pose environmental and health risks.

Conclusions

This study demonstrates that combined application of AMF and *Trichoderma* synergistically reduces CCN infestation in wheat through a coordinated, multi-layered mechanistic cascade. Microbial colonization enhances nutrient uptake, which primes metabolic defense pathways, including accumulation of sphingolipids, defense-related amino acids, and phenylpropanoid intermediates, and in turn drives transcriptomic reprogramming centered on SA-mediated signaling, collectively contributing to reduced nematode reproduction. Transcriptomic analysis identified PRB1-2 as a key regulatory hub in this response, with promoter, subcellular localization, and interaction data consistently supporting its induction via WRKY-mediated SA signaling under AMF + *Trichoderma* colonization. These findings position the AMF–*Trichoderma* consortium as effective, sustainable biocontrol agents and provide candidate genes for future crop improvement efforts.

Supplementary Information The online version contains supplementary material available at https://doi.org/10.1007/s00344-026-12331-8.

Acknowledgements The authors gratefully acknowledge the International Maize and Wheat Improvement Center (CIMMYT), Mexico, for providing financial support for this research. This study forms part of the Master's thesis of Özgenur Arslanoğlu, conducted under the supervision of Prof. Dr. Mustafa Imren and the co-supervision of Assistant Prof. Dr. Muhammad Sameeullah.

Author Contributions MS, MI and AAD designed the research. OA, AY, ND, and FU performed the experiments with the assistance of MS, MI and AAD. MS, MI, AAD and EY analyzed the data and wrote the manuscript.

Funding This work was supported by a grant from the International Maize and Wheat Improvement Center (CIMMYT), Mexico.

Declarations

Competing Interests The authors declare that they have no competing interests.

Ethical Approval and Consent to Participate Not applicable.

Consent for Publication Not applicable.

References

Alamri S, Nafady NA, El-Sagheer AM, El-Aal MA, Mostafa YS, Hashem M, Hassan EA (2022) Current utility of arbuscular

mycorrhizal fungi and hydroxyapatite nanoparticles in suppression of tomato root-knot nematode. Agronomy 12:671. https://doi.org/10.3390/agronomy12030671

Alcázar R, Altabella T, Marco F, Bortolotti C, Reymond M, Koncz C, Carrasco P, Tiburcio AF (2010) Polyamines: molecules with regulatory functions in plant abiotic stress tolerance. Planta 231:1237–1249. https://doi.org/10.1007/s00425-010-1130-0

Alexa A, Rahnenfuhrer J (2010) topGO: enrichment analysis for gene ontology. R package version 2 0. https://doi.org/10.18129/B9.bioc.topGO

Ashrafi S, Wennrich J-P, Becker Y, Maciá-Vicente JG, Brißke-Rode A, Daub M, Thünen T, Dababat AA, Finckh MR, Stadler M (2023) Polydomus karssenii gen. nov. sp. nov. is a dark septate endophyte with a bifunctional lifestyle parasitising eggs of plant-parasitic cyst nematodes (Heterodera spp). IMA Fungus 14:6. https://doi.org/10.1186/s43008-023-00113-w

Bibi H, Ur Rahim H, Anwar Khan A, Haris M, Iqbal M, Ali R, El-Sheikh MA, Kaushik P (2024) Harmonized tripartite approach: enhancing nutrient accessibility, uptake, and wheat productivity through Trichoderma harzianum, compost, and phosphorus synergy. J King Saud Univ Sci 36:103106. https://doi.org/10.1016/j.jksus.2023.103106

Bolger AM, Lohse M, Usadel B (2014) Trimmomatic: a flexible trimmer for Illumina sequence data. Bioinformatics 30:2114–2120. https://doi.org/10.1093/bioinformatics/btu170

Breiman A, Graur D (1995) Wheat evolution. Isr J Plant Sci 43:85–98. https://doi.org/10.1080/07929978.1995.10676595

Byrd DW Jr, Kirkpatrick T, Barker K (1983) An improved technique for clearing and staining plant tissues for detection of nematodes. J Nematol 15:142

Cacas J-L, Buré C, Grosjean K, Gerbeau-Pissot P, Lherminier J, Rombouts Y, Maes E, Bossard C, Gronnier J, Furt F et al (2015) Revisiting plant plasma membrane lipids in tobacco: a focus on sphingolipids. Plant Physiol 170:367–384. https://doi.org/10.1104/pp.15.00564

Covacevich F, Fernandez-Gnecco G, Consolo VF, Burges PL, Calo GF, Mondino EA (2025) Combined soil inoculation with mycorrhizae and Trichoderma alleviates nematode-induced decline in mycorrhizal diversity. Diversity 17:334. https://doi.org/10.3390/d17050334

Cristina Rodriguez MS, Petersen M, Mundy J (2010) Mitogen-activated protein kinase signaling in plants. Annu Rev Plant Biol 61:621–649. https://doi.org/10.1146/annurev-arplant-042809-112252

Dababat AE-FA, Sikora RA (2007) Influence of the mutualistic endophyte Fusarium oxysporum 162 on Meloidogyne incognita attraction and invasion. Nematology 9:771–776. https://doi.org/10.1163/156854107782331225

Ding T, Feng W, Bai M, Gu L, Duan T (2025) Arbuscular mycorrhizal fungi and Trichoderma longibrachiatum alter the transcriptome of Vicia villosa in response to infection by the fungal pathogen Stemphylium vesicarium. BMC Microbiol 25:86. https://doi.org/10.1186/s12866-025-03778-y

Dixon RA, Achnine L, Kota P, Liu C-J, Reddy MSS, Wang L (2002) The phenylpropanoid pathway and plant defence—a genomics perspective. Mol Plant Pathol 3:371–390. https://doi.org/10.1046/j.1364-3703.2002.00131.x

Dodds PN, Rathjen JP (2010) Plant immunity: towards an integrated view of plant–pathogen interactions. Nat Rev Genet 11:539–548. https://doi.org/10.1038/nrg2812

Durrant WE, Dong X (2004) Systemic acquired resistance. Annu Rev Phytopathol 42:185–209. https://doi.org/10.1146/annurev.phyto.42.040803.140421

El-Sharkawy HHA, Rashad YM, Ibrahim SA (2018) Biocontrol of stem rust disease of wheat using arbuscular mycorrhizal fungi and Trichoderma spp. Physiol Mol Plant Pathol 103:84–91. https://doi.org/10.1016/j.pmpp.2018.05.002

Fernandez-Gnecco G, Gégu L, Covacevich F, Consolo VF, Bouffaud M-L, Buscot F, Smalla K, Babin D (2024) Alone as effective as together: AMF and Trichoderma inoculation boost maize performance but differentially shape soil and rhizosphere microbiota. J Sustain Agric Environ 3:e12091

Gao X, Zhang K (2025) Enhancing iron and zinc uptake in spring wheat through commercial arbuscular mycorrhizal fungi inoculation under different soil phosphorus addition levels. Can J Soil Sci 105:1–10. https://doi.org/10.1139/cjss-2024-0049

Glazebrook J (2005) Contrasting mechanisms of defense against biotrophic and necrotrophic pathogens. Annu Rev Phytopathol 43:205–227. https://doi.org/10.1146/annurev.phyto.43.040204.135923

Graska J, Fidler J, Gietler M, Prabucka B, Nykiel M, Labudda M (2023) Nitric oxide in plant functioning: metabolism, signaling, and responses to infestation with Ecdysozoa parasites. Biology 12:927. https://doi.org/10.3390/biology12070927

Gustafson P, Raskina O, Ma X, Nevo E (2009) Wheat evolution, domestication, and improvement. In: Carver BF (ed) Wheat: science and trade. Wiley, Hoboken, pp 3–30. https://doi.org/10.1002/9780813818832.ch1

Guzmán-Guzmán P, Kumar A, de Los Santos-Villalobos S, Parra-Cota FI, Orozco-Mosqueda MC, Fadiji AE, Hyder S, Babalola OO, Santoyo G (2023) Trichoderma species: our best fungal allies in the biocontrol of plant diseases—a review. Plants 12:432. https://doi.org/10.3390/plants12030432

Han A-Q, Chen S-B, Zhang D-D, Liu J, Zhang M-C, Wang B, Xiao Y, Liu H-T, Guo T-C, Kang G-Z et al (2025) Effects of arbuscular mycorrhizal fungi on the growth and nutrient uptake in wheat under low potassium stress. Plants 14:1288. https://doi.org/10.3390/plants14091288

Hariharan G, Rifnas L, Prasannath K (2022) Role of Trichoderma spp. in biocontrol of plant diseases. In: Rai M, Bhatt D (eds) Microbial biocontrol: food security and post harvest management, vol 2. Springer, Cham, pp 39–78. https://doi.org/10.1007/978-3-030-87289-2_3

Hoagland DR, Arnon DI (1950) The water-culture method for growing plants without soil. University of California, Berkeley

Hooper DJ (1986) Extraction of free living stages from soil. In: Southey JF (ed) Laboratory methods for work with plant and soil nematodes. CAB International, London, pp 5–30

Hussain RMF, Sheikh AH, Haider I, Quareshy M, Linthorst HJM (2018) Arabidopsis WRKY50 and TGA transcription factors synergistically activate expression of PR1. Front Plant Sci 9:930. https://doi.org/10.3389/fpls.2018.00930

Kumar S, Zavaliev R, Wu Q, Zhou Y, Cheng J, Dillard L, Powers J, Withers J, Zhao J, Guan Z et al (2022) Structural basis of NPR1 in activating plant immunity. Nature 605:561–566. https://doi.org/10.1038/s41586-022-04699-w

Lebel E, Heifetz P, Thorne L, Uknes S, Ryals J, Ward E (1998) Functional analysis of regulatory sequences controlling PR-1 gene expression in Arabidopsis. Plant J 16:223–233. https://doi.org/10.1046/j.1365-313x.1998.00288.x

Li H, Xiao J, Gao Y-Q, Tang JJ, Zhang A-L, Gao J-M (2014) Chaetoglobosins from Chaetomium globosum, an endophytic fungus in Ginkgo biloba, and their phytotoxic and cytotoxic activities. J Agric Food Chem 62:3734–3741. https://doi.org/10.1021/jf500390h

Lopes A, Rivadavea W, Silva G (2024) Trichoderma secondary metabolites for effective plant pathogen control. Nanohybrid fungicides. Elsevier, Amsterdam, pp 239–255. https://doi.org/10.1016/B978-0-443-23950-2.00008-4

Martinus Oostenbrink M (1966) Major characteristics of the relation between nematodes and plants. Meded Landbouwhogesch Wageningen 66:1–46

McGonigle TP, Miller MH, Evans DG, Fairchild GL, Swan JA (1990) A new method which gives an objective measure of colonization

of roots by vesicular–arbuscular mycorrhizal fungi. New Phytol 115:495–501. https://doi.org/10.1111/j.1469-8137.1990.tb00476.x

Meng X, Zhang S (2013) MAPK cascades in plant disease resistance signaling. Annu Rev Phytopathol 51:245–266

Moreno-Lora A, Sousa-Ortega C, Recena R, Perea-Torres F, Delgado A (2023) Microbial inoculants improve nutrients uptake and yield of durum wheat in calcareous soils under drought stress in the Mediterranean region. Arch Agron Soil Sci 69:2233–2247

Naoumkina MA, Zhao Q, Gallego-Giraldo L, Dai X, Zhao PX, Dixon RA (2010) Genome-wide analysis of phenylpropanoid defence pathways. Mol Plant Pathol 11:829–846

Pariyar SR, Dababat AA, Nicol JM, Sikora RA (2010) Effect of different potting systems; inoculation time; nematode density and sources of cereal cyst nematode (Heterodera filipjevi) on juvenile penetration into wheat root system. Commun Agric Appl Biol Sci 75:479–485

Renčo M, Čermák V, Tománková K, Čudejková MM (2018) Morphological and molecular characterisation of Heterodera filipjevi (Madzhidov, 1981) from the Slovak Republic. Nematology 20:253–264

Robinson MD, McCarthy DJ, Smyth GK (2010) edgeR: a Bioconductor package for differential expression analysis of digital gene expression data. Bioinformatics 26:139–140

Sameeullah M, Sasaki T, Yamamoto Y (2013) Sucrose transporter NtSUT1 confers aluminum tolerance on cultured cells of tobacco (Nicotiana tabacum L). Soil Sci Plant Nutr 59:756–770. https://doi.org/10.1080/00380768.2013.830230

Sameeullah M, Demiral T, Aslam N, Baloch FS, Gurel E (2016) In silico functional analyses of SWEETs reveal cues for their role in AMF symbiosis. In: Hakeem KR, Akhtar MS (eds) Plant, soil and microbes. mechanisms and molecular interactions, vol 2. Springer, Cham, pp 45–58. https://doi.org/10.1007/978-3-319-29573-2_3

Sameeullah M, Yildirim M, Aslam N, Baloğlu MC, Yucesan B, Lössl AG, Saba K, Waheed MT, Gurel E (2021) Plastidial expression of 3β-hydroxysteroid dehydrogenase and progesterone 5β-reductase genes confer enhanced salt tolerance in tobacco. Int J Mol Sci 22:11736. https://doi.org/10.3390/ijms222111736

Schmelz EA, Huffaker A, Sims JW, Christensen SA, Lu X, Okada K, Peters RJ (2014) Biosynthesis, elicitation and roles of monocot terpenoid phytoalexins. Plant J 79:659–678

Schouteden N, De Waele D, Panis B, Vos CM (2015) Arbuscular mycorrhizal fungi for the biocontrol of plant-parasitic nematodes: a review of the mechanisms involved. Front Microbiol 6. https://doi.org/10.3389/fmicb.2015.01280

Sels J, Mathys J, De Coninck BM, Cammue BP, De Bolle MF (2008) Plant pathogenesis-related (PR) proteins: a focus on PR peptides. Plant Physiol Biochem 46:941–950

Shi X, Chen Q, Liu S, Wang J, Peng D, Kong L (2021) Combining targeted metabolite analyses and transcriptomics to reveal the specific chemical composition and associated genes in the incompatible soybean variety PI437654 infected with soybean cyst nematode HG1.2.3.5.7. BMC Plant Biol 21:217

Smiley RW, Dababat AA, Iqbal S, Jones MG, Maafi ZT, Peng D, Subbotin SA, Waeyenberge L (2017) Cereal cyst nematodes: a complex and destructive group of Heterodera species. Plant Dis 101:1692–1720

Smith SE, Facelli E, Pope S, Andrew Smith F (2010) Plant performance in stressful environments: interpreting new and established knowledge of the roles of arbuscular mycorrhizas. Plant Soil 326:3–20

Sodhi GK, Saxena S (2023) Plant growth-promoting endophyte Nigrospora oryzae mitigates abiotic stress in rice (Oryza sativa L). FEMS Microbiol Ecol 99:fiad094

Spagnoletti FN, Carmona M, Balestrasse K, Chiocchio V, Giacometti R, Lavado RS (2021) The arbuscular mycorrhizal fungus Rhizophagus intraradices reduces the root rot caused by Fusarium pseudograminearum in wheat. Rhizosphere 19:100369

Sun P, Huang Y, Yang X, Liao A, Wu J (2023) The role of indole derivative in the growth of plants: a review. Front Plant Sci 13:2022

Tsuda K, Katagiri F (2010) Comparing signaling mechanisms engaged in pattern-triggered and effector-triggered immunity. Curr Opin Plant Biol 13:459–465

Umer M, Anwar N, Mubeen M, Li Y, Ali A, Alshaharni MO, Liu P (2025) Roles of arbuscular mycorrhizal fungi in plant growth and disease management for sustainable agriculture. Front Microbiol 16. https://doi.org/10.3389/fmicb.2025.1616273

van Loon LC, Rep M, Pieterse CM (2006) Significance of inducible defense-related proteins in infected plants. Annu Rev Phytopathol 44:135–162

Vishwakarma SK, Ilyas T, Malviya D, Shafi Z, Shahid M, Yadav B, Singh UB, Rai JP, Singh H, Singh HV (2022) Arbuscular mycorrhizal fungi (AMF) as potential biocontrol agents. In: Rakshit A, Singh HB, Singh AK, Singh US, Fraceto L (eds) Rhizosphere microbes: biotic stress management. Springer, Singapore, pp 197–222

Wang L, Yan X, Tang Z (2024a) Joint impacts of Meloidogyne incognita and soil nutrition on Solanum lycopersicum var. cerasiforme. Plant Dis 108:1252–1260

Wang X, Zhang S, Xu B (2024b) Characterization of the serine protease TlSP1 from Trichoderma longibrachiatum T6 and its function in the control of Heterodera avenae in wheat. J Fungi 10. https://doi.org/10.3390/jof10080569

Weng W, Yan J, Zhou M, Yao X, Gao A, Ma C, Cheng J, Ruan J (2022) Roles of arbuscular mycorrhizal fungi as a biocontrol agent in the control of plant diseases. Microorganisms 10. https://doi.org/10.3390/microorganisms10071266

Yan Y, Mao Q, Wang Y, Zhao J, Fu Y, Yang Z, Peng X, Zhang M, Bai B, Liu A et al (2021) Trichoderma harzianum induces resistance to root-knot nematodes by increasing secondary metabolite synthesis and defense-related enzyme activity in Solanum lycopersicum L. Biol Control 158:104609

Yeken MZ (2023) Investigation of genotype × environment interactions for the seed mineral composition in Phaseolus vulgaris L. J Food Compos Anal 124:105657

Yu G, Wang L-G, Han Y, He Q-Y (2012) clusterProfiler: an R package for comparing biological themes among gene clusters. OMICS 16:284–287

Zeng H-Y, Yao N (2022) Sphingolipids in plant immunity. Phytopathol Res 4:20

Zhang S, Gan Y, Xu B, Xue Y (2014) The parasitic and lethal effects of Trichoderma longibrachiatum against Heterodera avenae. Biol Control 72:1–8

Zhang S, Gan Y, Ji W, Xu B, Hou B, Liu J (2017a) Mechanisms and characterization of Trichoderma longibrachiatum T6 in suppressing nematodes (Heterodera avenae) in wheat. Front Plant Sci 8:2017

Publisher's Note Springer Nature remains neutral with regard to jurisdictional claims in published maps and institutional affiliations.

Springer Nature or its licensor (e.g. a society or other partner) holds exclusive rights to this article under a publishing agreement with the author(s) or other rightsholder(s); author self-archiving of the accepted manuscript version of this article is solely governed by the terms of such publishing agreement and applicable law.